

## Pressure Fluctuations on the Surface of Two Circular Cylinders in Tandem Arrangement\*

by Masaru MORIYA\*\* and Hiroshi SAKAMOTO\*\*

(Received September 25, 1985)

### Abstract

The fluctuating pressures on the surfaces of two circular cylinders of the same diameter in a tandem arrangement were measured in the subcritical region in order to obtain the distributions of their r. m. s. values of lift and drag coefficient as a function of the spacing between the two cylinders. The spacing ranged from 2.0 to 6.0 diameters. Also, the time histories of the fluctuating lift and drag coefficients could be obtained by a conditional sampling technique. The results strongly suggested that the r. m. s. pressure and the r. m. s. lift force increased in a step-like manner at the critical spacing where vortex shedding will just occur from the upstream cylinder. The r. m. s. value of the fluctuating lift coefficient was much larger than that of the drag coefficient for the upstream and downstream cylinders.

### 1. Introduction

The interference of flow around two circular cylinders has been extensively studied by many investigators. However, there is very little reported to show the surface-pressure fluctuations and fluctuating fluid forces. Authors have already reported the r. m. s. pressure distributions on the surface of cylinders and the spanwise and circumferential pressure correlations between two points<sup>1)</sup>. They yielded information about the spanwise coherence of the fluctuating drag and lift forces and properties of r. m. s. fluctuating forces.

In this paper, the properties of the fluctuating pressure on the surface of two circular cylinders in a tandem arrangement are presented in some detail for various different spacings between the cylinders. Measurements are mainly made of fluctuating fluid forces acting on the cylinders, and the fluctuating fluid forces are evaluated using the conditional sampling technique.

### 2. Experimental apparatus and procedure

The experimental work was carried out in a closed-circuit wind tunnel which has 0.5 m × 0.5 m cross section and a 2.5 m long rectangular test section. Time-mean velocity distributions were measured at several cross sections ahead of the upstream cylinder by means of a Pitot-static tube. Flow two-dimensionality at the test section was well maintained with 6.2 d (d: diameter of the circular cylinder) from the center plane of the wind tunnel and the nonuniformity was

\* Presented at the 23th Hokkaido regional meeting of the JSME (September, 1981), Kitami

\*\* Department of Mechanical Engineering, Kitami Institute of Technology.

less than 1%. The free-stream velocity in this experiment was maintained constant at  $U_\infty = 20 \pm 0.2$  m/s and the r. m. s. longitudinal velocity fluctuation was about 0.4% of the approach velocity.

The downstream and upstream cylinders tested were machined brass and aluminum respectively with 49 mm diameter,  $d$ , with a smooth surface finish. The cylinders were placed at the test section at right angles to the approach flow, and the clearance between the cylinders and the wind tunnel walls was sealed with "O" rings. The flow blockage due to the presence of the cylinder is 9.8% in area. A 0.8 mm diameter pressure tap was located at the center of the span to measure the time-mean pressure on the surface of the cylinder by Betz type manometer with its accuracy of 0.2 mmAq. And time-mean pressure distribution was obtained by rotating the cylinder every 10 degrees from 0 to 180 degrees.

Also the fluctuating pressure on the surface of the cylinder was measured by a semiconductor pressure transducer. The pressure sensing element was installed inside the cylinder with a small cavity between the opening of the tap and the diaphragm of the transducer. The pressure transducer responded to pressure fluctuation up to 500 Hz with a gain factor of  $1 \pm 0.06$ , the phase lag being negligible. This frequency was well above the frequencies of vortex shedding from the upstream and downstream cylinders.

In order to evaluate the fluctuating forces, first ensemble averaging of the fluctuating pressure on the circumference of the cylinder for each angular position was conducted. Then the ensemble-averaged time variation of pressure along the circumference on the surface of the cylinder was obtained from each phase. The fluctuating forces can be calculated from integration of the ensemble-averaged time variation of pressure along the circumference.

### 3. Results and Discussion

A deft sketch of two cylinders in a tandem arrangement is shown in Fig. 1. The diameter of the cylinders is denoted by  $d$  and the distance between their centers by  $l$ . The angle measured from the front stagnation point is written as  $\theta$  for the upstream and downstream cylinders. The Reynolds number  $R (=U_\infty d/\nu)$  was maintained at  $9.0 \times 10^4$  throughout the present experiment.

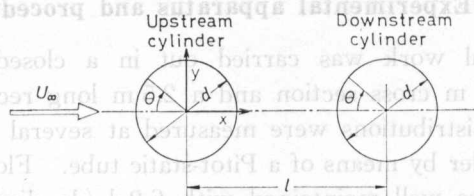


Fig. 1. Two circular cylinders in a tandem arrangement.

#### 3.1 Time-mean pressure, drag and Strouhal number

The time-mean pressure distributions on the surface of the upstream and

downstream cylinders are presented in Fig. 2 for several nondimensional spacings  $l/d$ . These results are seen to agree fairly well with other investigators<sup>1,2)</sup>. The time-mean drag coefficients  $C_D$  for the upstream and downstream cylinders versus  $l/d$  are plotted in Fig. 3 together with those obtained by Arie et al.<sup>1)</sup> and Okajima<sup>3)</sup> respectively at approximately the same Reynolds number.

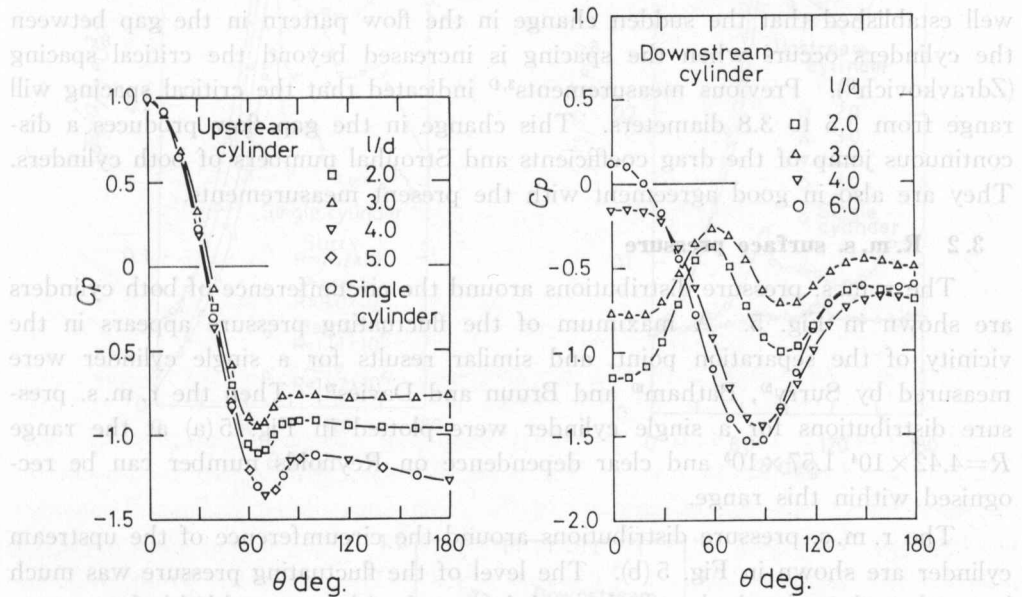


Fig. 2. Time-mean pressure distribution on the surface of (a) upstream and (b) downstream cylinder.

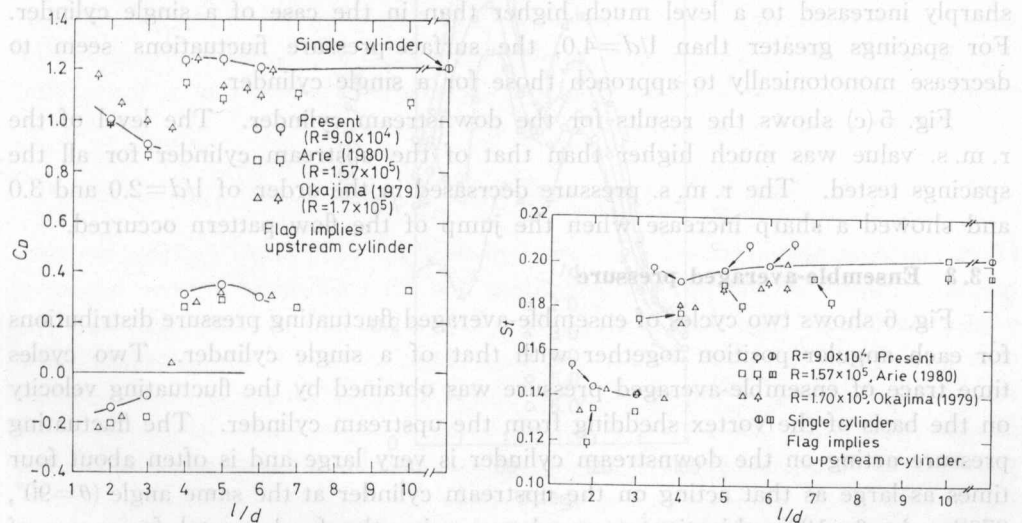


Fig. 3. Time-mean drag coefficient plotted against nondimensional spacing  $l/d$ .

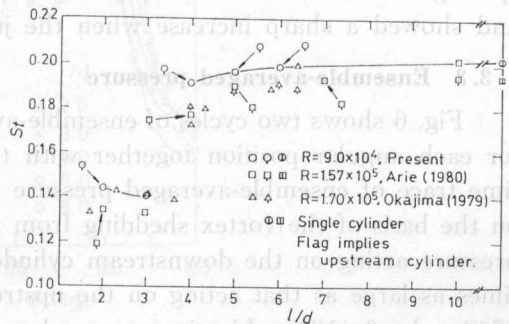


Fig. 4. Strouhal number plotted against nondimensional spacing  $l/d$ .

The vortex shedding frequency was determined on the basis of the power spectrum of the surface-pressure fluctuation, i.e. the frequency corresponding to a spectrum peak. The results are shown in Fig. 4 in the form of the Strouhal number  $S_t$  versus  $l/d$ . The Strouhal number are seen to be almost the same. Also, the results of the present experiment agree with Arie's<sup>1)</sup> and Okajima's<sup>3)</sup> data taken at Reynolds number  $R=1.57 \times 10^5$  and  $1.7 \times 10^5$ , respectively. It is well established that the sudden change in the flow pattern in the gap between the cylinders occurs when the spacing is increased beyond the critical spacing (Zdravkovich<sup>4)</sup>). Previous measurements<sup>3,4)</sup> indicated that the critical spacing will range from 3.5 to 3.8 diameters. This change in the gap flow produces a discontinuous jump of the drag coefficients and Strouhal numbers of both cylinders. They are also in good agreement with the present measurements.

### 3.2 R. m. s. surface pressure

The r. m. s. pressure distributions around the circumference of both cylinders are shown in Fig. 5. A maximum of the fluctuating pressure appears in the vicinity of the separation point, and similar results for a single cylinder were measured by Surry<sup>5)</sup>, Batham<sup>6)</sup> and Bruun and Davies<sup>7)</sup>. Then the r. m. s. pressure distributions for a single cylinder were plotted in Fig. 5(a) at the range  $R=4.42 \times 10^4$ – $1.57 \times 10^5$  and clear dependence on Reynolds number can be recognised within this range.

The r. m. s. pressure distributions around the circumference of the upstream cylinder are shown in Fig. 5(b). The level of the fluctuating pressure was much lower than that of a single cylinder and decreased with increased  $l/d$  before vortex shedding from the upstream cylinder occurred, i.e. for  $l/d < 3.5$ . Immediately after the occurrence of the vortex shedding ( $l/d=4.0$ ), however, the r. m. s. pressures sharply increased to a level much higher than in the case of a single cylinder. For spacings greater than  $l/d=4.0$ , the surface-pressure fluctuations seem to decrease monotonically to approach those for a single cylinder.

Fig. 5(c) shows the results for the downstream cylinder. The level of the r. m. s. value was much higher than that of the upstream cylinder for all the spacings tested. The r. m. s. pressure decreased in the order of  $l/d=2.0$  and  $3.0$  and showed a sharp increase when the jump of the flow pattern occurred.

### 3.3 Ensemble-averaged pressure

Fig. 6 shows two cycles of ensemble-averaged fluctuating pressure distributions for each angular position together with that of a single cylinder. Two cycles time trace of ensemble-averaged pressure was obtained by the fluctuating velocity on the basis of the vortex shedding from the upstream cylinder. The fluctuating pressure acting on the downstream cylinder is very large and is often about four times as large as that acting on the upstream cylinder at the same angle ( $\theta=90^\circ$ ,  $270^\circ$ ). At  $\theta=180^\circ$ , this time trace shows twice the fundamental frequency of vortex shedding, and also the phase turn over at  $\theta=90^\circ$  and  $270^\circ$  for both cylinders.

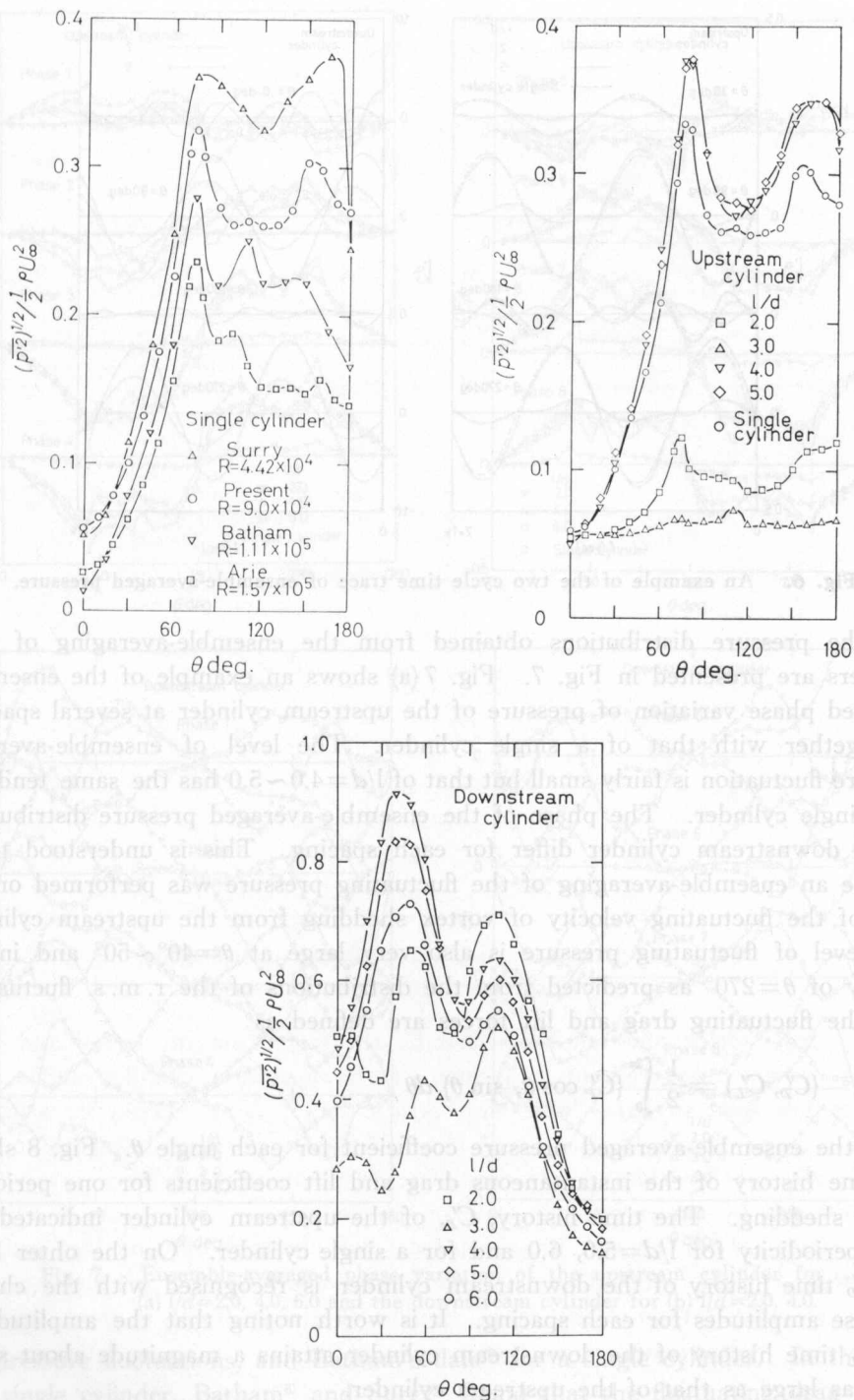


Fig. 5. R. m. s. surface-pressure distribution of (a) single, (b) upstream and (c) downstream cylinder.



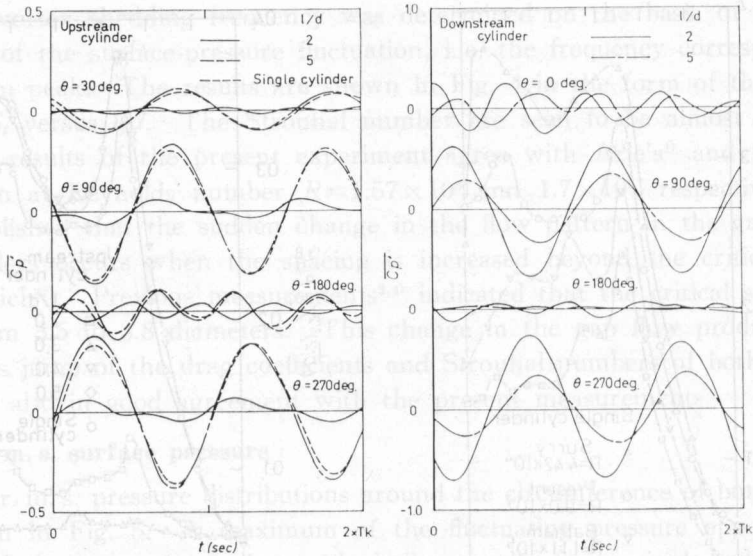


Fig. 6. An example of the two cycle time trace of ensemble-averaged pressure.

The pressure distributions obtained from the ensemble-averaging of both cylinders are presented in Fig. 7. Fig. 7(a) shows an example of the ensemble-averaged phase variation of pressure of the upstream cylinder at several spacings  $l/d$  together with that of a single cylinder. The level of ensemble-averaged pressure fluctuation is fairly small but that of  $l/d=4.0\sim 5.0$  has the same tendency as a single cylinder. The phase of the ensemble-averaged pressure distributions of the downstream cylinder differ for each spacing. This is understood to be because an ensemble-averaging of the fluctuating pressure was performed on the basis of the fluctuating velocity of vortex shedding from the upstream cylinder. The level of fluctuating pressure is also very large at  $\theta=40^\circ\sim 50^\circ$  and in the vicinity of  $\theta=270^\circ$  as predicted from the distributions of the r. m. s. fluctuation.

The fluctuating drag and lift forces are defined as

$$\{C'_D, C'_L\} = \frac{1}{2} \int_0^{2\pi} \{\bar{C}'_p \cos \theta, \sin \theta\} d\theta$$

$\bar{C}'_p$  is the ensemble-averaged pressure coefficient for each angle  $\theta$ . Fig. 8 shows the time history of the instantaneous drag and lift coefficients for one period of vortex shedding. The time history,  $C'_D$ , of the upstream cylinder indicated the clear periodicity for  $l/d=5.0, 6.0$  and for a single cylinder. On the other hand the  $C'_D$  time history of the downstream cylinder is recognised with the change of those amplitudes for each spacing. It is worth noting that the amplitude of the  $C'_L$  time history of the downstream cylinder attains a magnitude about seven times as large as that of the upstream cylinder.

The r. m. s. drag and lift coefficients evaluated from the time history of  $C'_D$  and  $C'_L$  are presented in Fig. 9. These experimental measurements are compared with Arie's measurements<sup>1)</sup> obtained from the circumferential correlation of sur-

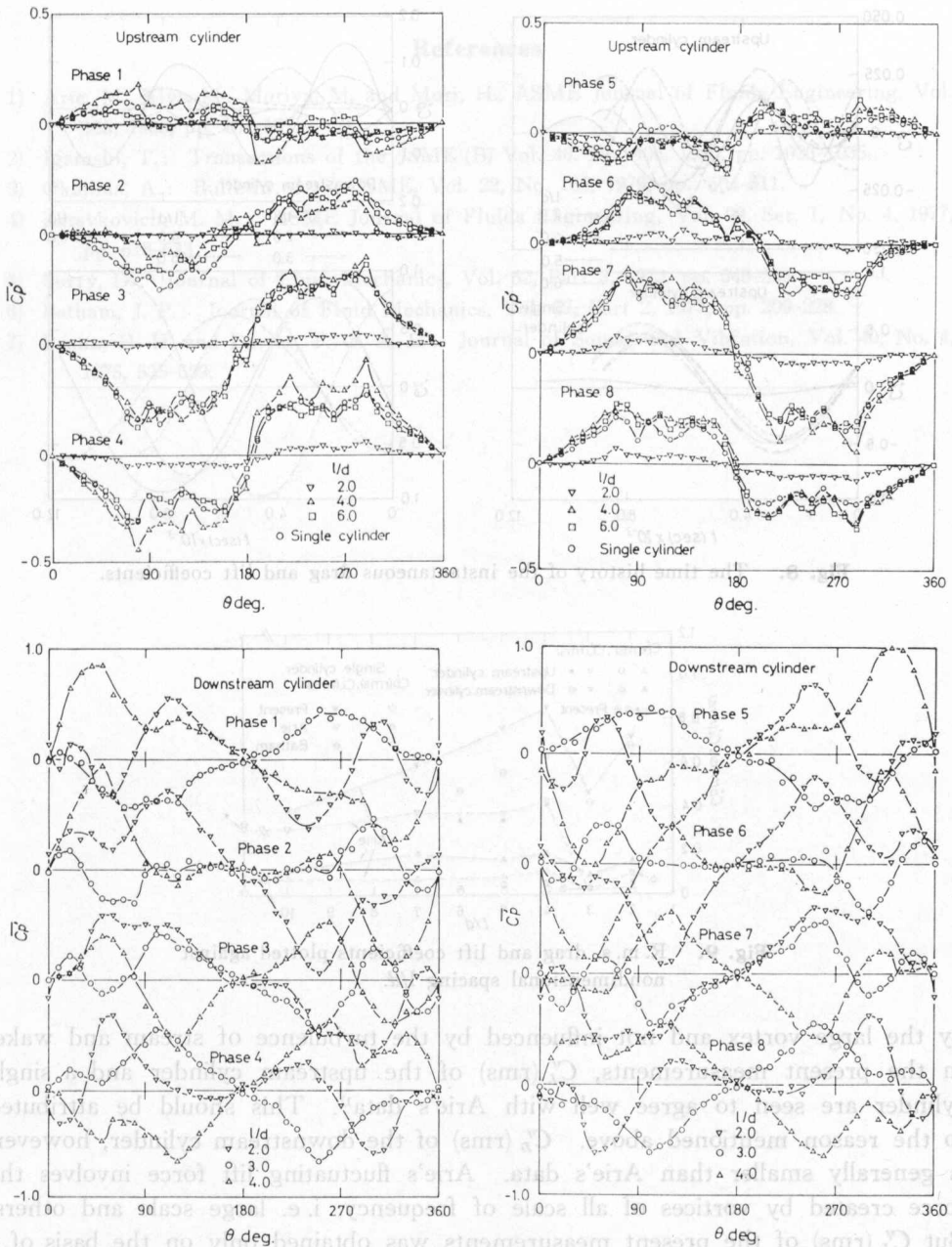


Fig. 7. Ensemble-averaged phase variation of the upstream cylinder for (a)  $l/d=2.0, 4.0, 6.0$  and the downstream cylinder for (b)  $l/d=2.0, 4.0$ .

face-pressure fluctuations, and Batham's data<sup>6</sup> for a single cylinder. In the case of a single cylinder, Batham<sup>6</sup> and Surry<sup>7</sup> found that the fluctuating drag varied with the turbulent stream whereas the fluctuating lift was affected very little by the turbulent stream in comparison with the fluctuating drag force. This was interpreted to mean that the major part of the fluctuating lift force was generated

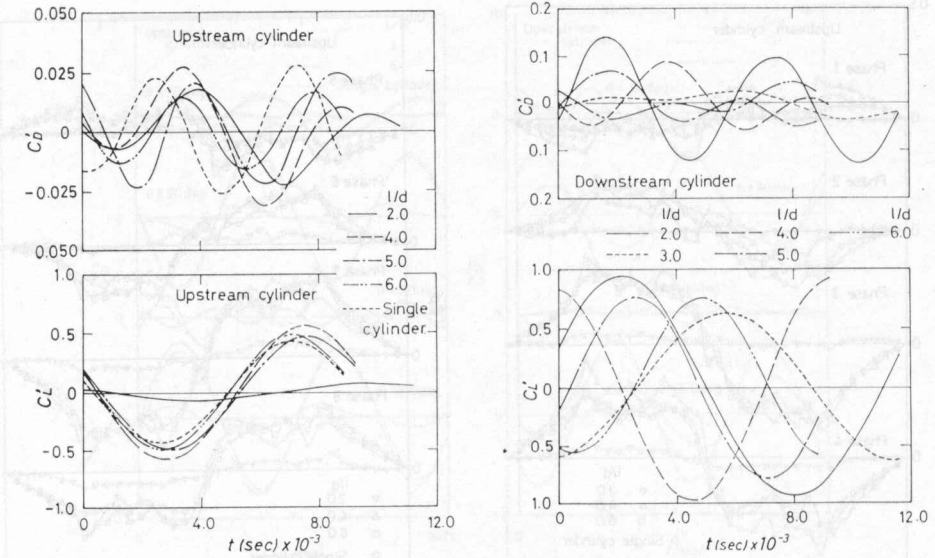


Fig. 8. The time history of the instantaneous drag and lift coefficients.

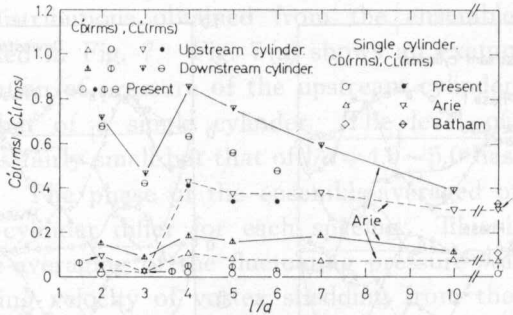


Fig. 9. R. m. s. drag and lift coefficients plotted against nondimensional spacing  $l/d$ .

by the large vortex and not influenced by the turbulence of stream and wake. In the present measurements,  $C'_L$  (rms) of the upstream cylinder and a single cylinder are seen to agree well with Arie's data<sup>11</sup>. This should be attributed to the reason mentioned above.  $C'_D$  (rms) of the downstream cylinder, however, is generally smaller than Arie's data. Arie's fluctuating lift force involves the force created by vortices of all scale of frequency, i. e. large scale and others. But  $C'_L$  (rms) of the present measurements was obtained only on the basis of a large scale vortex. Accordingly, it is understandable that the pressure measurements are smaller than Arie's data. Similar comments apply to the  $C'_D$  (rms) of the present measurements.

### Acknowledgements

The authors express their sincere thanks to Mr. Y. Obata and Mr. K. Abe for their assistance in the construction of the experimental apparatus.



## References

- 1) Arie, M., Kiya, M., Moriya, M. and Mori, H., ASME Journal of Fluids Engineering, Vol. 105, 1980, pp. 161-167.
- 2) Igarashi, T.: Transactions of the JSME (B) Vol. 46, No. 406, 1980, pp. 1026-1035.
- 3) Okajima, A.: Bulletin of the JSME, Vol. 22, No. 166, 1979, pp. 504-511.
- 4) Zdravkovich, M. M.: ASME Journal of Fluids Engineering, Vol. 99, Ser. I, No. 4, 1977, pp. 618-633.
- 5) Surry, D.: Journal of Fluid Mechanics, Vol. 52, Part 3, 1972, pp. 543-563.
- 6) Batham, J. P.: Journal of Fluid Mechanics, Vol. 57, Part 2, 1973, pp. 209-228.
- 7) Bruun, H. H. and Davies, P. O. A. L.: Journal of Sound and Vibration, Vol. 40, No. 4, 1975, 535-559.

### The Characteristics of Cycle-to-Cycle Combustion Variation in a Diesel Engine with Alcohol Blended Fuel

by Takaochi YAMADA, Hiroshi ISHIBASHI, Hideyuki TSUNEMOTO,  
Noboru MIYAMOTO and Tadashi MURAYAMA

This paper presents the characteristics of cycle-to-cycle combustion variations in a diesel engine. The combustion variations are particularly significant for low cetane fuels like alcohol, and cause deterioration in thermal efficiency as well as rough running. Combustion variations appear in various forms, such as variations in ignition lag, mean effective pressure, maximum combustion pressure, or combustion rate. These variations are largely caused by the variable ignition lag. This paper also reports the characteristics of CPE related to combustion noise in relation to combustion variations.

### し　ま　え　が　き

アルコール燃料が用いられるようになって以来、内燃機関においてはエンジン性能の向上、新材料の開発、あるいは代替燃料の使用に対する試みなど多大な努力が積み重ねられている。代替燃料としては、生産性の容易さからメタノールが、また自動車などのリサイクル資源利用の面からエタノールが有望視され、ここ数年、ガソリン機関およびディーゼル機関を問わずこれらの使用に関する調査が積極的に行なわれるようになってきた。従って、これまでアルコール燃料

昭和58年10月10日東京大学工学部機械系研究室にて一般発表(昭和58年3月)

山田孝典、山田孝典、山田孝典以上、東京大学工学部機械系研究室

山田孝典、山田孝典、山田孝典以上、東京大学工学部機械系研究室